Science Journal of Chemistry
2019; 7(1): 1-10
http://www.sciencepublishinggroup.com/j/sjc
doi: 10.11648/j.sjc.20190701.11
ISSN: 2330-0981 (Print); ISSN: 2330-099X (Online)

Mineralogy, Physical and Mechanical Properties of Adobes Stabilized with Cement and Rice Husk Ash

Issiaka Sanou[1], Mohamed Seynou[2, *], Lamine Zerbo[2], Raguilnaba Ouedraogo[2]

[1]Department of Biologicals Sciences, University Nazi BONI, Bobo Dioulasso, Burkina Faso

[2]Department of Chemistry, University Ouaga I Pr Joseph KI-ZERBO, Ouagadougou, Burkina Faso

Email address:
seynou1mohamed@yahoo.fr (M. Seynou)

[*]Corresponding author

To cite this article:
Issiaka Sanou, Mohamed Seynou, Lamine Zerbo, Raguilnaba Ouedraogo. Mineralogy, Physical and Mechanical Properties of Adobes Stabilized with Cement and Rice Husk Ash. *Science Journal of Chemistry.* Vol. 7, No. 1, 2019, pp. 1-10. doi: 10.11648/j.sjc.20190701.11

Received: November 25, 2018; **Accepted**: December 20, 2018; **Published**: January 24, 2019

Abstract: A Burkina Faso clay referenced SAB has been characterized to be used as raw material in the making of adobes. Mineralogical studies (by XRD, DTA-TG), chemical and geotechnical studies (Atterberg limits, particle size distribution) carried out on this clay have shown that it is composed of kaolinite (62 wt%), quartz (30 wt%) and goethite (18 wt%). It is a sandy-silty clay of medium plasticity containing no swelling minerals. Its particles are mainly clay (19 wt%), silt (36 wt%), fine and coarse sand (45 wt%). It is thus suitable for the development of adobes for habitats. The adobes elaborated with SAB clay have been stabilized with an optimal cement content of 10 wt%, which offers a mechanical strength greater than 2 MPa; minimum value for single-level constructions. In order to improve the physical properties (density, porosity, water absorption by capillarity, erosion resistance, compressive and flexural strengths) of these adobes and to reduce cement consumption as much as possible, the cement (10 wt%) was partially or totallysubstitutedby rice husk ash. This substitution contributed to the improvement of the physical and mechanical properties of the adobes, due on the one hand to the effect of micro-filling of the ash and on the other hand to the increase of the CSH resulting from the pozzolanic reactivity between the released portlandite by the hydration of the cement and the amorphous silica of the rice husk ash.

Keywords: Clay, Adobe, Cement, Rice Husk Ash and Pozzolanic Activity

1. Introduction

More than 1/3 of the world's population live in mud buildings or houses [1]. In Africa more than 2/3 of the population live in this type of house. This type of habitat, also called green habitat, is ecological and respects the environment [2, 3]. It requires less energy for its implementation and for their thermal comfort. Good moisture regulators and good acoustic insulators, the mud bricks are suitable for many types of construction and are the most accessible in the developing countries. Despite these multiple benefits, mud habitats have low durability due to poor mechanical quality and poor water performance [4-6]. This is the situation that the people of Saaba, rural district of Ouagadougou (Burkina Faso) in the peri-urban area, are living. This rural district with a very high population density and non-parceled areas, is built mainly with raw earth. The district has a potential clay soil site which is currently exploited by the vast majority of the population for the manufacture of adobe bricks. Buildings are short-lived and require permanent repair, especially after each rainy season (Figure 1). This difficult situation makes the living conditions of the populations even more precarious.

An alternative solution is then necessary to improve the quality of bricks from this clay soil. Cement stabilization is possible but with a low proportion in view of the non-accessibility of cement by these people.

To reduce the amount of cement and at the same time improve the durability of the bricks that will be made, some of the cement has been substituted by active pozzolan. The accessibility of pozzolan led us to think about rice husks as regards the main agricultural activity of the populations. The present work then presents the results of stabilization of the Saaba clay soil for the construction of a raw brick by the pozzolan-cement additions. Emphasis is placed on the

mechanical and water performance of stabilized bricks. The mineralogical evolution of these bricks with the additions has been also explored.

Figure 1. *(a) Site of Saaba exploited for the manufacture of adobes, (b) a building and adobes bricks from Saaba site, (c) a ruin building of Saaba site after rainy season.*

2. Materials and Experimental Methods

2.1. Materials

The clay raw material used for the development of the adobes is a clay from Burkina Faso taken in the rural district of Saaba in Ouagadougou (12°22'21,7'' North and 1°26'30,9'' West). This site is heavily exploited by the inhabitants for the making of adobes. This clay will be referenced SAB in the rest of the work. The particle size distribution of the sample is accessed after wet sieving for the coarser fraction (≥ 80 µm) according to NF 94-056 standard [7] and by sedimentation for the fine fraction (< 80 µm) according to NF 94-057 standard [8]. The particle size distribution (Table 1) deduce from the curve of the Figure 2 shows that the SAB clay is composed of 55% fines (clay + silt). This fine fraction plays the key role of binder between the larger grains (45%) which will constitute the skeleton of the bricks that will be issued. The Atterberg limits (Table 1) determined according to standard NF P94-051 [9] indicate that the sample is a moderately plastic clay soil. This average plasticity is in agreement with the granulometric composition made of fine and coarse. The Atterberg limits of SAB are in the spindle of the land plasticity indices usable for raw bricks (Figure 3). The methylene blue value of 1.43 g / 100 g obtained from standardNF P 94-068 [10] shows that SAB belongs to the category of sandy-silty soils, which is sensitive to water. The geotechnical properties of SAB confer a possibility of using it for the production of adobes.

The rice husk used in this study was taken from the village of Bama, located a few kilometers from the town of BoboDioulasso in western Burkina Faso. In this village rice activity is very developed and can supply a large part of the population of western Burkina with rice. The rice husk that is a by-product is then available in very large quantities and is used in some places as fuel. The rice husk ash (RHA) was produced by calcining at 680°C the rice husk for five hours with a heating rate of 10°C/min. The choice of these parameters was made from literature data to avoid the formation of a large amount of carbon, which could compromise the pozzolanic activity of the material [11].

The cement used in this study for the various tests comes from Diamond Cement, a cement factory in Burkina Faso. It is a CEM I 45 cement whose chemical, physical and mineralogical properties are recorded in Table 2 [12].

Table 1. *Geotechnical parameters ofSAB's clay.*

Particle size distribution		**Atterberg's limits**	
Class	%	Liquid limit W_L (%)	42
Coarse sand (> 200 µm)	24	Plasticity limit W_P (%)	22
Fine sand (20 – 200 µm)	21	Plasticity index P_I (%)	20
Slit (2 - 20 µm)	36	Methylene Blue Value (g/100g)	
Clay (< 2 µm)	19	1.43	

Table 2. *Chemical and mineralogical composition and some physicals properties of cement use.*

Chemical composition (Wt. %)	**SiO_2**	**Al_2O_3**	**Fe_2O_3**	**MgO**	**CaO**	**P_2O_5**	**SO_3**	**Na_2O**	**K_2O**	**FL**	**IR**	**LOI**
	20.12	**5.73**	**4.06**	**1.18**	**64.8**	**0.39**	**2.68**	**0.08**	**0.17**	**0.8**	**0.28**	**0.27**
Mineralogy (Wt. %)	C_3S			C_2S			C_3A			C_4AF		
	55.7			15.68			8.31			12.34		
Physicalproperties	Specificdensity			Apparent Density			Setting time (h)					
	3.02			1.06			3					

F. L: Free lime I. R : Insoluble residues LOI: Loss on ignition (1000°C)

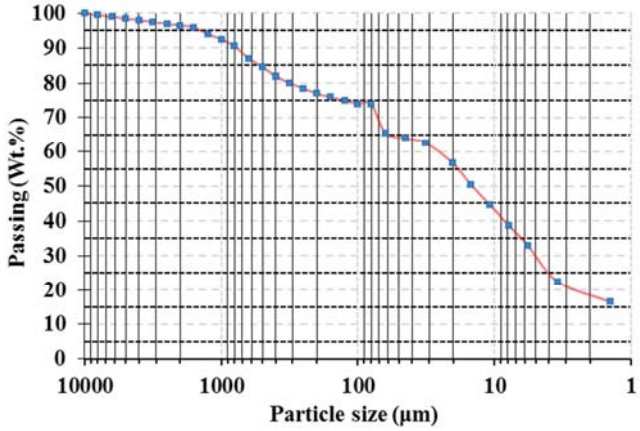

Figure 2. *Particle size distribution of SAB'sclay.*

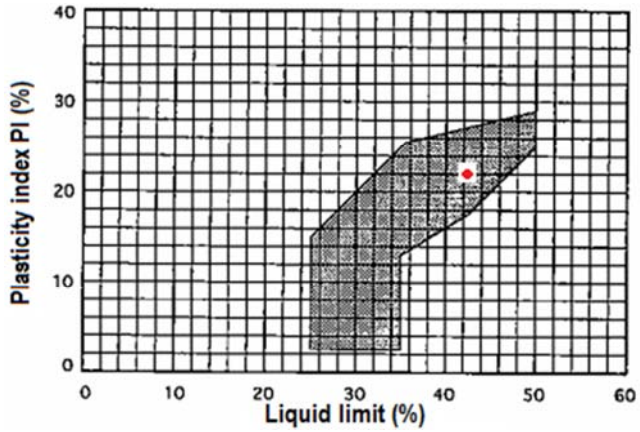

Figure 3. *Position of SAB's clay in CRATerre-EAG diagram.*

2.2. Experimental Methods

The mineralogy of the raw materials and the adobes formulated was performed by X-ray diffraction (XRD), infra-red spectroscopy (IR) and differential thermal and thermogravimetric analysis (DTA/TG). The diffractometer used is a Bruker AXS, operating at 40 kV – 40 mA and employing a graphite monochromatic CuKα radiation. The infrared spectra were recorded in the range of 400 - 4000 cm^{-1} using a Perkin Elmer FT-IR Spectrometer. The thermal analysis (DTA/TG) was carried out using SETARAM instrument operating at 10°C/min from ambient to 1200°C. Calcined alumina was taken as a reference.

The chemical composition of the raw clay materials was assessed by Inductively Coupled Plasma - Atomic Emission Spectrometry (ICP-AES). The loss on ignition was evaluated by sample calcination up to 1000°C.

The mineralogical composition of raw sample was obtained by using XRD and results of chemical analyses. For a chemical element "a", the equation 1 [13] was used to calculated the amount T(a) of oxide.

$$T(a)=\Sigma MiPi(a) \quad (1)$$

Where M_i is the amount (in wt.%) of mineral i in the material under study; P_i (a) is the proportion of element a in the mineral i.

The pozzolanic activity index is the ratio of the mechanical compressive strength at 28 days of the specimens containing pozzolan and those containing none known as reference specimens [14]. The formulation of the specimens was made according to standard NF-P-15-403 [15]. The preparation of the adobes begins with the grinding of the SAB clay earth to a particle size less than 1 mm. After grinding, different mixtures are prepared and homogenized to dryness. Following homogenization, a sufficient amount of water is added to have the right and same consistency for all mixtures. The kneading is done manually, the mixture obtained is introduced into a prismatic mould 4x4x16 cm^3. The mould is then covered with plastic and then kept in the shade. After removal from the mould, the bricks obtained are stored in order to undergo the various tests after a minimum duration of 28 days.

The density of adobes was measured by the method of hydrostatic weighing according to standard NF P94-053 [16]. As for the Closed porosity (P) of the adobes, it has been deduced from the density by equation 2 [17].

$$P(\%) = (1-\frac{d_a}{d_s})\times 100 \quad (2)$$

Where d_a is the apparent density and d_s the absolute density.

The water performance of the bricks is evaluated by the water absorption test and the rain erosion test. The water absorption test is intended to determine the amount of water absorbed by capillarity of the adobes. The tests were conducted using the AFPC-AFREM protocol [18]. This test consists in measuring the increase in the mass of the specimen placed in a receptacle whose water level is 5 mm above the lower face of the specimen. The erosion resistance test consists in dropping drops of water for 10 minutes, under a pressure of 2 bars on bricks placed on a stand at an angle of 30° to the vertical [6]. The bricks are then dried in the sun for a few hours and then baked at 105 ° C for 24 hours. After the parboiling, the masses of the bricks are determined. The mass

percentage of degraded adobe (D) is then evaluated from the equation 3.

$$D(\%) = \frac{m_1 - m_2}{m_1} x100 \quad (3)$$

With: m_1: mass of the raw brick and m_2: mass of the degraded brick.

The compressive and flexural strength are the mechanical parameters of the bricks that have been evaluated. The flexural strength is carriedout on the 4x4x16 cm^3 adobes with a hydraulic press equipped with a 200 kN load cell at a controlled displacement rate of 0.5 mm/min. Theequation 4 makes it possible to determinethe limit stress in flexural strength [19].

$$\sigma(MPa) = \frac{3FE}{2le^2} \quad (4)$$

F is the intensity of the force applied, E is the distance between the two specimen supports, *l* is the width of the specimens, e is its thickness and σ is the stress at break.

In order to determine the compressive strength, the half-prism resulting from the flexural strength is subjected to a monotonously increasing load until breaking. Thus, the compressive strength is the ratio of the breaking load to the cross section of the specimen. The value of the resistance R_c is obtained from the equation 5.

$$R_c = \frac{P}{S} \quad (5)$$

With: S: average value of the section in cm^2 and P the load in kN. The flexural and compression strength tests are carried out in accordance with standard NF P 15-471 [20].

3. Results and Discussion

3.1. Characterization of Raw Materials

The XRD pattern of SAB clay (Figure 4) shows that it consists essentially of quartz, kaolinite and goethite. The analysis of the SAB thermograms presented in Figure5 makes it possible to identify thermal phenomenon characteristic of the phases identified by the XRD.

The first endothermic peak at 78°C corresponds to the remove of adsorbed water which is associated with a loss of mass of 0.61 wt%. The second endothermic peak at 330°C. corresponds to the dehydroxylation of goethite in hematite. This transformation is associated with a loss of 1.04 wt%. The third endothermic peak at 538°C corresponds to the dehydroxylation of kaolinite to metakaolinite [21]. This peak is the largest and is associated with this loss of mass of 7.68 wt%. The 575°C hook corresponds to the allotropic transformation of quartz α to quartz β [22]. Finally, the only exothermic peak split at 973°C corresponds to the structural reorganization of metakaolinite and spinel phase and primary mullite.

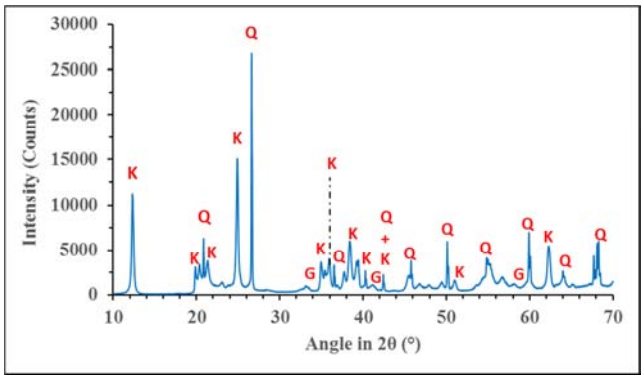

K: Kaolinite, Q: Quartz and G: Goethite

Figure 4. *X-ray diffraction pattern of SAB's clay.*

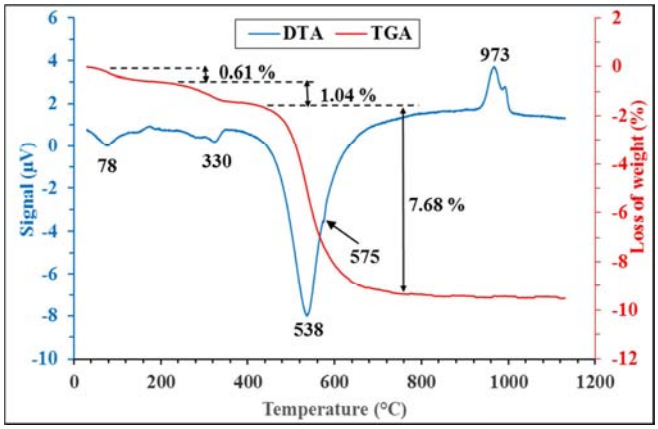

Figure 5. *Thermograms DTA-TGA of SAB's clay.*

The chemical composition (Table 3) shows that SAB is mainly composed of silica and alumina with relatively high proportion of iron oxide. These results corroborate the results of the mineralogical analysis.

From the results of chemical analysis and X-ray diffraction, the mineral phases reported in Table 3 were quantified using theequation 1. SAB is a mixture of plasticizer and degreaser suitable for making bricks. The absence of swelling minerals such as montmorillonite in SAB is an asset for the developmentof mud bricks.

The chemical composition of the rice husk ash (RHA) recorded in Table 3 shows that it consists mainly of silica of 96.84 wt% in weight. This value is slightly higher than that given by the literature, which sets a maximum of 96 wt% in weight of silica [23]. The RHA is low in alkalis because the sum of the alkaline oxides Na_2O and K_2O of 0.84 wt% is lower than the minimum value of 0.95 wt% fixed in the literature [23]. Moreover, the sum of the oxides SiO_2, Al_2O_3 and Fe_2O_3 is greater than 70 wt%, which is the minimum value required for a pozzolanic material according to ASTM standard C-618 [24]. The glass content (SiO_2 - CaO) of 96.37 wt% is well above the minimum value of 34 wt%. These results suggest that rice husk ash is a very reactive pozzolan [24]. The total of analyzedoxides (99.98 wt%) shows that the RHA contains no carbon or is in trace form. This low carbon content of RHA improves its pozzolanic reactivity [25]. The presence of significant amounts of carbon in the materials is

the source of pore formation, and negatively influences the durability of the processed materials [26]. The X-ray pattern of RHA (Figure 6) has a broad hump (halo) centered at about 22°(2θ) indicating the presence of amorphous phases. Silica, the main element of the rice husk ash, is then in amorphous form and will confer a good pozzolanic reactivity of the RHA [27]. The pozzolanic index determined at 28 days cure with 25 wt% replacement of cement by RHA is 135 wt%. This value exceeds the minimum of 75 wt% required by ASTM C-618 for a pozzolanic material [24]. This high-performance result of RHA is related to its essentially amorphous silica composition and the absence of carbon.

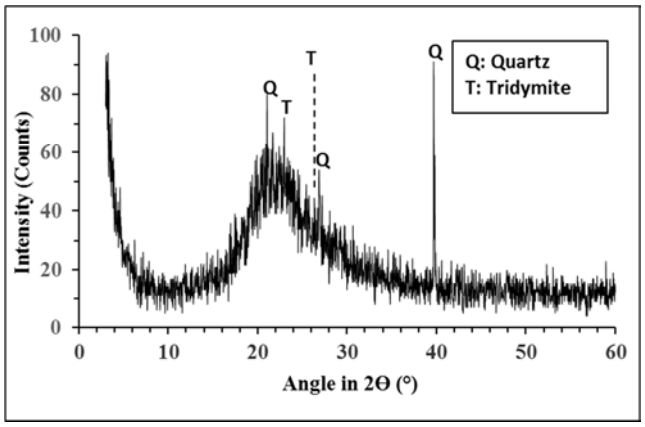

Figure 6. *X-ray diffraction pattern of RHA.*

Table 3. *Chemical and mineralogical composition of SAB clay and RHA.*

Chemical composition (wt.%)			Mineralogy of SAB's clay	
Oxide	**SAB'sclay**	**RHA**	**Mineral**	**wt.%**
SiO_2	59.38	96.84	Kaolinite	62
Al_2O_3	24.64	1.03		
Fe_2O_3	5.36	0.38		
TiO_2	0.47	0.1	Quartz	30
Na_2O	0.08	0.03		
MgO	0.08	0.32		
K_2O	0.10	0.81	Goethite	6
CaO	0.04	0.47		
LOI	9.68	-		
Total	99.83	99.98	Balance	2

3.2. Optimization of the Cement Content

Before the addition of pozzolan, the optimum cement content needed to improve the mechanical strength of the SAB bricks was determined. The mechanical compressive strength of the bricks with 0 to 12 wt% cement additions was followed. The results shown in Figure 7 show a small and gradual improvement in strength with additions of up to 8 wt% cement. These resistances still remain below the minimum value of 2 MPa required by the XP 13-901 standard [28]. Beyond the 8 wt% cement content, the compressive strength of adobes is significantly improved with values above the norm. Between 10 and 12 wt% of cement resistance seems to stabilize with a very small variation. Taking into account these results and the economic and ecological aspect (less cement possible), the 10wt% cement content constitutes a reasonable content for the formulation of the adobes.

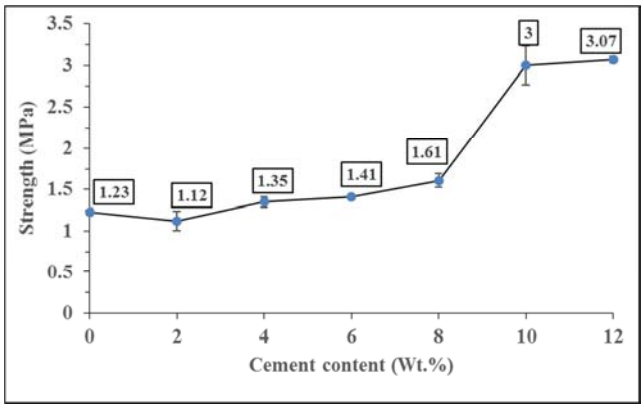

Figure 7. *Compressive strength of adobes stabilized with cement.*

3.3. Influence of the Cement-RHA Mixture on the Mineralogy of the Adobes

To follow the influence of RHA on the mineralogy, the physical and mechanical properties of the adobes, new formulations were made in the proportions shown in Table 4.

Table 4. *Composition of mixtures.*

References	Composition
C_{10}	10 wt% cement + 0% wt RHA
B_2	8 wt % cement + 2 wt% RHA
B_4	6 wt % cement + 4 wt% RHA
B_6	4 wt% cement + 6% wt RHA
B_8	2 wt% cement + 8% wt RHA
B_{10}	0 wt% cement + 10% wt RHA

The mineralogy of the adobes was followed by X-ray diffraction and infra-red spectroscopy. The analysis of infra-red spectrum (Figure 8) shows a presence of phases of the raw material and new phases. Kaolinite by its vibration bands $\nu_{Al\text{-}OH}$ and $\nu_{Si\text{-}O\text{-}Al}$ and quartz by its vibration bands $\nu_{Si\text{-}O}$ and $\nu_{Si\text{-}O\text{-}Si}$, are the main detected phases from the SAB material [29]. The bands around 875 and 1430 cm^{-1} detected in the adobes containing cement-RHA are characteristic of calcite ($CaCO_3$) [30]. Calcite is formed as a result of a carbonation reaction involving portlandite produced by hydration of the cement and carbon dioxide from the atmosphere according to reaction 1. These two bands decrease in intensity with the increase of the RHA content in adobe. This decrease is explained on the one hand by the dilution effect of the cement which produces less portlandite by its hydration and on the other hand by the probable recovery of the portlandite by the RHA by pozzolanic reaction according to the reactions 2, 3 and 4 [31]. The broadband around 3400 cm^{-1} is attributed to both the hydration water and the hydroxyl vibration of hydrated calcium silicate (CSH) [32]. The CSH gels are derived on the one hand from the hydration of the alite (C_3S) and belite (C_2S) compounds of the cement (reaction 5 and 6) [32]and on the other hand from the pozzolanic reaction (reaction 4). The X-ray diffraction pattern (figure 9) confirms the disappearing of calcite in adobes with RHA.

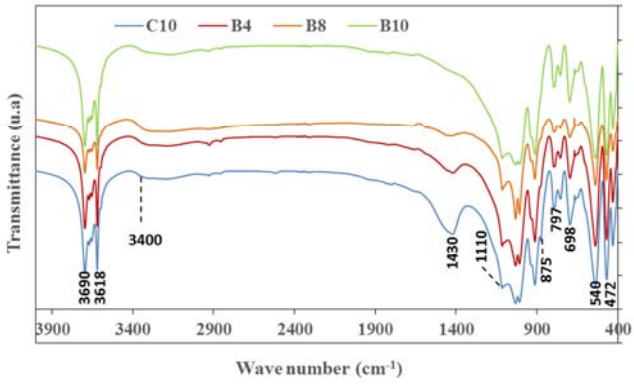

Figure 8. *Infrared spectrum of adobes.*

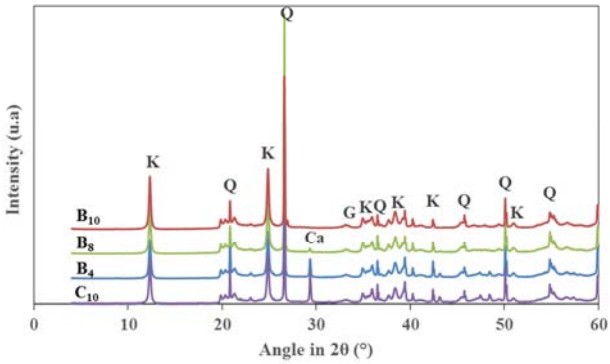

K: Kaolinite, Q: Quartz, G: Goethite and Ca: Calcite.

Figure 9. *X-ray diffraction pattern of adobes.*

$Ca(OH)_2 + CO_2 \rightarrow CaCO_3 + H_2O$ (reaction 1)

$Ca(OH)_2 \leftrightarrow Ca^{2+} + 2\ OH^-$: dissolution of portlandite (reaction 2)

SiO_2 (amorphous silica of RHA) + 2 OH- (hydroxyl of portlandite) $\rightarrow H_2SiO_4^{2-}$(reaction 3)

$xCa^{2+} + H_2SiO_4^{2-} + 2(x\text{-}1)OH^- + (y–x)H_2O \rightarrow (CaO)_x(SiO_2)(H_2O)_y\ [C_xSH_y]$ (reaction 4)

$2\ C_3S + 6\ H \rightarrow C_3S_2H_3$ (CSH) + 3 CH (reaction 5)

$2\ C_2S + 4\ H \rightarrow C_3S_2H_3$ (CSH) + CH (reaction 6)

Where H stands for H_2O, C_3S for 3CaO. SiO_2, C_2S for 2CaO. SiO_2 and CH for portlandite.

3.4. Influence of the Cement-RHA Mixture on the Physical and Mechanical Properties of the Adobes

The evolution of apparent density and closed porosity are illustrated inFigure 10. As the RHA level increases, the density decreases up to 6 wt%. Beyond the 6 wt% content, the density increases. This same observation was made by Hossain and Mol [33] in their study on the stabilization of clay soils with natural pozzolana and industrial wastes. For these authors, the densification of the material depends on the grain size distribution of the raw material and the stabilizer. Initially the stabilizers cover the raw material to form large sets which consequently occupy large spaces. This will result in a decrease in density until the stabilizer compensates the wide spaces. Thus, adobe containing 10 wt% RHA has the highest density (1.51). This value is higher than that obtained by Sutas and al [34], they indeed obtained a density of about 1.42 for bricks also containing 10 wt% of RHA. The adobe containing only the RHA is denser, therefore apparently less porous than those obtained by substitution of the cement by the RHA. In all cases, the decrease in density must be associated with the increase in macroporosity. As for the porosity, it evolves in the opposite direction of the density.

The linear shrinkage of the adobes after drying at 90 (Figure 11) days increases slowly with the RHA content up to 6 wt% of RHA. Beyond 6 wt% of RHA, shrinkage increases rapidly with RHA content reaching 6 wt% with adobes containing only RHA. These results corroborate the density results. The fine particles of the RHAs, in the absence of cement infiltrate the porosity of the adobe and allows a high densification.

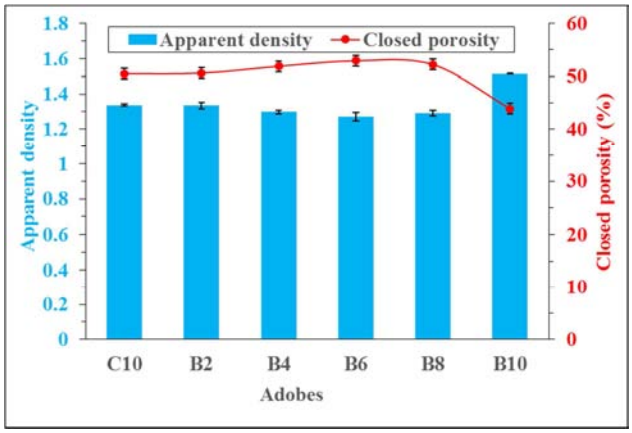

Figure 10. *Apparent density and closed porosity.*

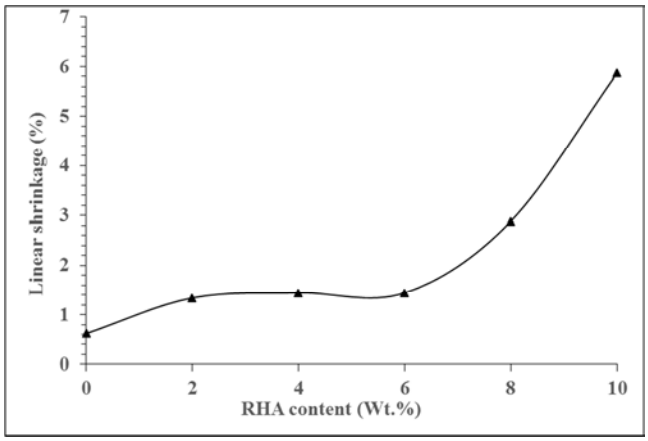

Figure 11. *Linear shrinkage of adobes.*

The mechanical strengths in flexural as in compressive (Figure 12) increase with the percentage of substitution of cement by the RHA, up to 4 wt%. Adobes containing 4wt% of RHA exhibit the best mechanical strengths in both flexural and compressive. Beyond the 4 wt% content, the partial replacement of cement by the RHA reduces the mechanical strength. However, with 10 wt% of RHA, an increase in mechanical strength is observed. The incorporation of RHA into the matrix contributes to the mechanical performance of adobes by combining its pozzolanic activity and its high capacity for micro filling. These two phenomena strongly

modify the microstructure of adobe and therefore its physical and mechanical properties. At young ages the filling effect takes precedence over the pozzolanic activity. For adobes of more than 90 days of cure, the pozzolanic activity participates more in the mechanical resistance than the filling effect for suitable contents. Several authors have obtained the best mechanical strength for substitution rates around 20 – 30 wt% of cement by RHA [25, 35]. The adobes B2 and B4 with respectively 2 wt% and 4 wt% substitution of the 10 wt% of cement respectively correspond to a substitution of 20 wt% and 40 wt% of the cement and are then at best close to the optimal content proposed by the authors. This optimal activity combined with the particle filling effect gives B4 the best resistance. The portlandite has been consumed to form a surplus of CSH and the amount of pores is reduced. Beyond the 4 wt% replacement (B6 and B8) the resistance of adobes decreases. This regression is strongly dependent on the one hand on the dilution effect of the cement and the low pozzolanic activity on the other hand. Dilution due to cement substitution with high levels of RHA reduces the amount of CSHfrom cement hydration. It is the same for the amount of portlandite released, which causes a low pozzolanic activity. The mechanical strength is then more governed by the filling effect. Without the cement, the pore-filling effect of pores by RHA is important and permits to obtain dense adobes with appreciable mechanical resistance.

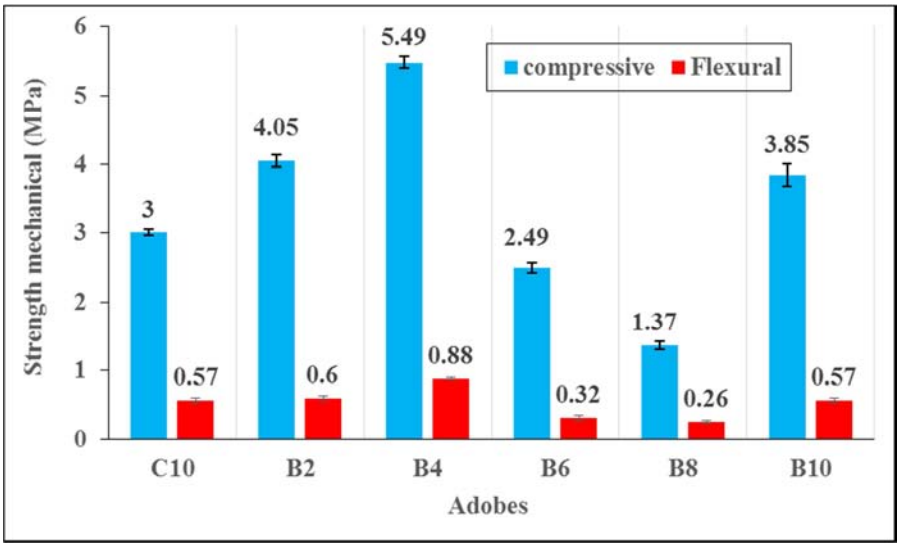

Figure 12. *Flexural and Compressive strength of adobes.*

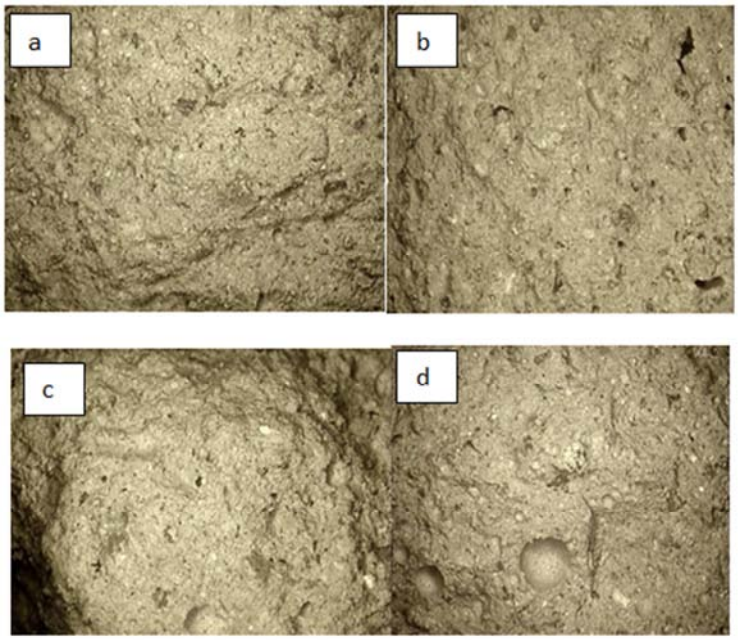

Figure 13. *Video microscopy images:(a) adobe C10, (b) adobe B2,(c)adobe B4,(d)adobe B10.*

The video microscopy images (Figure 13) of the adobe breaking facies show a similarity at the level of the microstructure of B4 and B10 with however a few micro pores at B4. The microstructure of B10 shows a nearly filled material without pores.

3.5. Influence of the Cement-RHA Mixture on the Water Performance of Adobes

The Figure 14 shows the results of water absorption by capillarity. The water absorption coefficient decreases with the percentage of RHA. Thus, adobe containing 10 wt% RHA (without cement) has the lowest absorption coefficient (0.494 kg. $m^{-2}s^{-1/2}$). This suggests that the presence of RHA in adobe makes it less porous. As a result, the adobe hardly absorbs water, which leads to a decrease in the absorption coefficient. This performance of the bricks would be due to the filler effect of the ashes. In fact, the RHA particles, because of their fine sizes, can be inserted between the grains of the clay matrix. This favours the narrowing of the pore size. This decrease in the water absorption coefficient with the increase in the RHA content is also related to the decrease in the amount of cement. The presence of cement increases the absorption of water because, even after 21 days of cure of adobes, the hydration of the cement continues thus inducing a demand for water. Under the effect of rain, the adobes can undergo disaggregation more or less pronounced depending on their quality. The impact of rain on different adobes was evaluated by the erosion test by artificial rain. The results obtained according to the mass losses are shown in figure 15. Adobes B8 and B10 with less or no cement have the largest mass losses. Thus, the degradation of adobes (Figure 16) containing no cement at levels of at least 4wt% is important. This degradation of the adobes could be due to the absence of cement binder in a sufficient quantity. Actually, during hydration of the cement, there is production of hydrated calcium silicates (CSH). These CSHs play the role of glue and unify the aggregates between them to form a rigid material [17, 36]. With the dilution of the cement content by the addition of RHA, the amount of CSH is also reduced and thus exposes the adobes to erosion with rain. The adobes B2 and B4 despite the dilution are not affected because the pozzolanic reactivity in these adobes is optimal and produces additional CSH that compensate for the dilution effect. The pore-filling effect of the RHA makes it possible to obtain appreciable compressive strengths by closing the pores without the creation of proper bonds between the particles. This lack of bonding is responsible for water degradation.

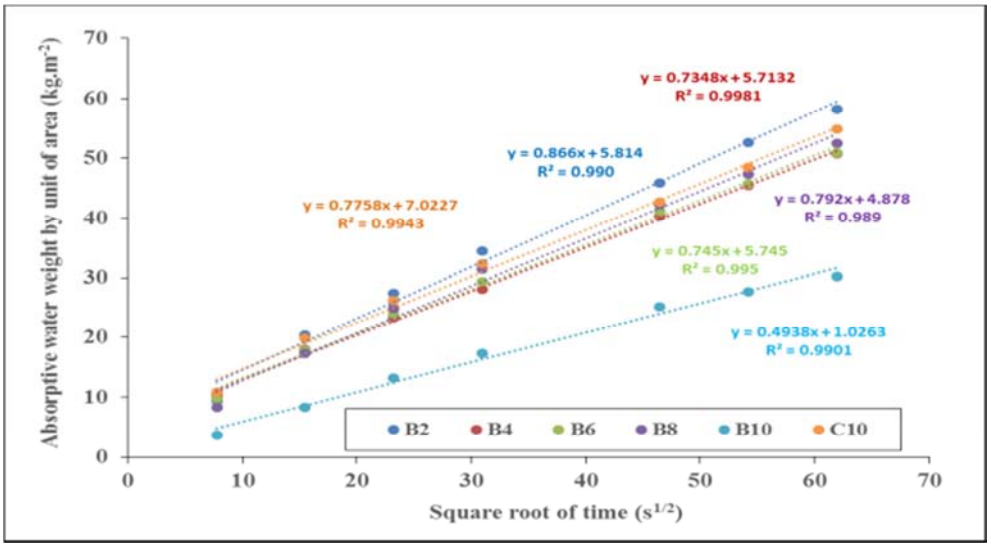

Figure 14. *Mass of absorbed water par unit area of adobes versus time.*

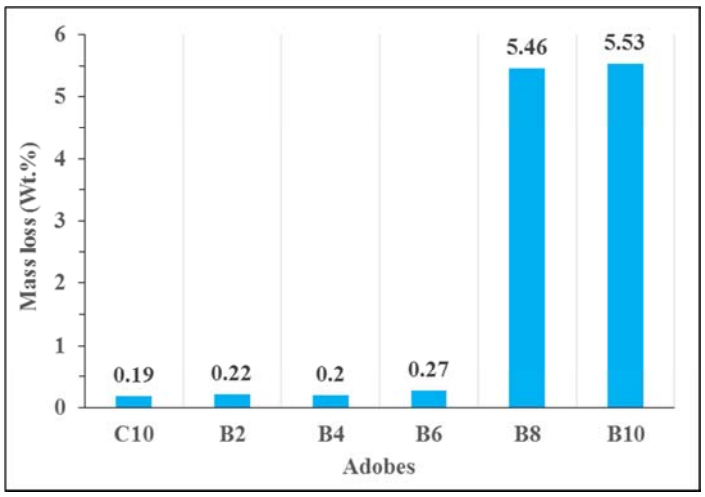

Figure 15. *Mass loss of adobes after the rain erosion test.*

Figure 16. *Adobes images: (a) before rain erosion test and (b) after the rain erosion test.*

4. Conclusions

The adobes made from sandy-loamsoil at the Saaba site have been stabilized using cement and ashes from calcined rice husks. The optimum cement content for the production of the adobes is 10 wt% by mass. A progressive replacement of the cement by the RHA modify the mineralogy of the adobes by the presence of CSH and improve their physical and mechanical properties.

Thus, the adobes containing 4 wt% pozzolan have the best mechanical strengths in both flexural and compressive. Thus, the adobe formulation from Saaba clay soil can be amended to cement and RHA in proportions of 6 wt% cement and 4 wt% RHA. These amendments use less cement and improve the mechanical strength and erosion resistance of the adobes.

Acknowledgements

We are grateful to Younoussa Millogo of University Nazi BONI of Burkina Faso for his implication in the characterization of samples and for his advice during the writing of this article.

References

[1] Binici H., Aksogan O., Shah T.(2005) Invertigation of fibre reinforced mud bricks as a building material. Construction and Building Materials 19, 313-318.

[2] Kouakou C. H., Morel J. C. (2009) Strength and elasto-plastic properties of non-industrial building materials manufactured with clay as a natural binder. Applied Clay Science 44,27-34.

[3] Pagliolico S. L., Ronchetti S., Turcato E. A., Bottino G., Gallo L. M., Depaoli R. (2010) Physicochemical and mineralogical characterization of earth for building in North West Italy. Applied Clay Science 50, 439-454.

[4] Vilane B. R. T (2010) Assessment of stabilization of adobes by confined compression test. Biosystems Engineering 106, 551-558.

[5] Adormi E., Coïsson E., Ferretti D. (2013) In situ Characterization of archaeological adobe bricks. Construction and Building Materials 40, 1-9.

[6] Millogo Y., Morel J. C., Aubert J-E., Ghavami K. (2014) Experimental analysis of pressed Adobe Blocks reinforced with Hibiscus cannabinus fibers. Construction and Building Materials 52, 71-78.

[7] NF P18-056 (1978) Analyse granulométrique par tamisage. AFNOR.

[8] NF P94-057 (1992) Analyse granulométrique des sols, méthode par sédimentation. AFNOR.

[9] NF P94-051 (1993) Détermination des limites d'Atterberg.

[10] NF P 94-068 (1993) Mesure de la quantité et de l'activité de la fraction argileuse. Détermination de la valeur de bleu de méthylène d'un sol par essai à la tâche. AFNOR.

[11] Venkatanarayanan H. K, Rangaraju P. R (2015) Effect of grinding of low carbon rice husk ash on the microstructure and performance properties of blended cement concrete. Cement and concrete composites 55, 348-363.

[12] Millogo Y., Hajjaji M., Ouedraogo R., Gomina M.(2008) Cement-lateritic gravels mixtures: microstructure and strength characteristics, Construc. Build. Mater. 22, 2078-2086.

[13] Yvon J., Garin P., Delon J. F, cases J. M. (1982) Valorisation des argiles kaolinitiques des Charentes dans le caoutchouc naturel. Bulletin de Minéralogie 105, 431-437.

[14] Donatello S., Tyrer M., Cheeseman C. R (2010) Comparison of test methods to assess pozzolanic activity. Cement and Concrete Composites 32, 121-127.

[15] NF P15-403 (1996) "Sable normal et mortier normal" AFNOR-Paris.

[16] NF P94-053 (1991) Détermination de la masse volumique des sols fins en laboratoire.

[17] Dao K., Ouedraogo M., Millogo Y., Aubert J-E., Gomina M.(2018) Thermal, hydric and mechanical behaviours of adobes stabilized with cement. Construc. Build. Mater. 158, 84-96.

[18] AFPC-AFREM (1997) Durabilité des bétons-Mésure de l'absorption d'eau par capillarité.

[19] Seynou M., Ouedraogo R., Millogo Y., Traore K., Bama B. C. A. (2009) Geotechnical, mineralogical, chemical and mechanical characterization of clay raw material from Korona (Burkina Faso). Journal de la Société Ouest Africaine de Chimie 27, 9-19.

[20] NF P15-471 (1990) Méthodes d'essais des ciments: Détermination des résistances mécaniques AFNOR-Paris.

[21] Chakchouk A., Trifi L., Samet B., Bouaziz S. (2009) Formulation of blended cement: effect of process variables on clay pozzolanic activity. Construction and Building Materials 23, 1365-1373.

[22] Millogo Y., HajjajiM., Morel J. C. (2011) Physical properties, microstructure and mineralogy of termite mound material considered as construction materials. Applied Clay Science 52, 160-164.

[23] Harish K. V., Rangaraju P. R. (2013) Material characterization studies on low-and high-carbon rice husk ash and their performance in Portland cement mixtures. Advances in Civil Engineering Materials 2(1), 266-287.

[24] Norme, ASTM Standard, C 618(2008) Standard Specification for coal Fly Ash and Raw or Calcined Natural Pozzolan for Use in Concrete, West Conshohocken, PA: Annual Book of ASTM standards, ASTM International.

[25] Cordeiro G. C., Filho R. D. T., Fairbairn E. M. R. (2009) Use of ultrafine rice husk ash withhigh-carbon content as pozzolan in high performance concrete. Materials and structures 42, 983-992.

[26] Nehdi M., Duquette J., Damatty A. E. (2003) Performance of rice husk ash produced using a new technology as a mineral admixture in concrete. Cement and Concrete Research 33 (8), 1203-1210.

[27] Erika Y. N., Moisés F., Sagrario M-R, Sérgio F. S, Michelle S. R., Olga R., Holmer S. J. (2014)Charaterisation and properties of elephant grass ashes as supplementary cementing material in pozzolan/$Ca(OH)_2$ pastes. Construction and Building Materials 73, 391-398.

[28] XP P 13-901 (2001) Blocs de terre comprimée pour murs et cloisons: Définitions Spécifications-Méthodes d'essais-Conditions de réception.

[29] Sore S. O., Messan A., Prud'homme E., Escadeillas G., Tsobnang F. (2018) Stabilization of compressed earth blocks (CEBs) by geopolymer binder based on local materials from Burkina Faso. Construction and Building Materials 165, 333-345.

[30] Dias C. M. R., Cincotto M. A., Savastano J. H., John V. M. (2008) Long-term aging of fiber-cement corrugated sheets, The effect of carbonation, leaching and rain. Cem. Concr. Compos. 21, 255-265.

[31] Millogo Y., Hajjaji M., Ouédraogo R. (2008) Microstructure and physical properties of lime clayey-adobe bricks. Construction and Building Materials 22, 2386-2392.

[32] Millogo Y., Morel J. C (2012) Microstructural characterization and mechanical properties of cement stabilized adobes. Materials and structures 45, 1311-1318.

[33] Hossain K. M. A., Mol L. (2011) Some engineering properties of stabilized clayey sols incorporating natural pozzolans and industrial wastes. Construction and building Materials 25, 3495-3501.

[34] Sutas J., Mana A., Pitak L. (2012) Effect of Rice Husk Ash to Properties of Bricks. Procedia Engineering 32, 1061-1067.

[35] Saraswathy V., Song H (2007)Corrosion performance of rice husk ash blended concrete. Construction and building Materials 21, 1779-1784.

[36] Medhat S., Ayman M. K. (2014) Engineering and mineralogical characteristics of stabilized unfired montmorillonic clay bricks. HBRC Journal 10, 82-91.